

## Review of Recent Searches for Rare and Forbidden Dilepton Decays of Charmed Mesons

David A. Sanders

*Department of Physics and Astronomy, University of Mississippi-Oxford, 122 Lewis Hall  
University, MS 38677, USA*

I briefly review the results of recent searches for flavor-changing neutral current and lepton-flavor and lepton-number violating decays of  $D^+$ ,  $D_s^+$ , and  $D^0$  mesons (and their antiparticles) into modes containing muons and electrons. The primary focus is the results from Fermilab charm hadroproduction experiment E791. E791 examined 24  $\pi\ell\ell$  and  $K\ell\ell$  decay modes of  $D^+$  and  $D_s^+$  and  $\ell^+\ell^-$  decay modes of  $D^0$ . Limits presented by E791 for 22 rare and forbidden dilepton decays of  $D$  mesons were more stringent than those obtained from previous searches,<sup>1</sup> or else were the first reported.

*Keywords:* Charm, Rare, Forbidden, Decay, Dilepton

### 1. Introduction

Searches for rare and forbidden decays allow investigation of physics beyond the Standard Model and of phenomena in mass ranges beyond those available to current accelerators. One way to search for physics beyond the Standard Model is to examine decay modes that are forbidden or else are predicted to occur at a negligible level (rare). Observing such decays would constitute evidence for new physics, and measuring their branching fractions would provide insight into how to modify our theoretical understanding, e.g., by introducing new particles or new gauge couplings. These new mediators could include: leptoquarks, horizontal gauge bosons, or something even more esoteric.

This review focuses on recent results from the Fermilab experiment E791<sup>2</sup> search for 24 decay modes of the neutral and charged  $D$  mesons (which contain the heavy charm quark). These decay modes\* fall into three categories:

- (i) FCNC – flavor-changing neutral current decays ( $D^0 \rightarrow \ell^+\ell^-$  and  $D_{(d,s)}^+ \rightarrow h^+\ell^+\ell^-$ , in which  $h$  is either a  $\pi$  or  $K$ );
- (ii) LFV – lepton-flavor violating decays ( $D^0 \rightarrow \mu^\pm e^\mp$ ,  $D_{(d,s)}^+ \rightarrow h^+\mu^\pm e^\mp$ , and  $D_{(d,s)}^+ \rightarrow h^-\mu^+e^+$ , in which the leptons belong to different generations);

\*Charge-conjugate modes are included implicitly throughout this paper.

- (iii) LNV – lepton-number violating decays ( $D_{(d,s)}^+ \rightarrow h^- \ell^+ \ell^+$ , in which the leptons belong to the same generation but have the same sign charge).

Decay modes belonging to (i) occur within the Standard Model via higher-order diagrams, but estimated branching fractions<sup>3</sup> are  $10^{-8}$  to  $10^{-6}$ . Such small rates are below the sensitivity of current experiments. However, if additional particles such as supersymmetric squarks or charginos exist, they could contribute additional amplitudes that would make these modes observable. Decay modes belonging to (ii) and (iii) do not conserve lepton number and thus are forbidden within the Standard Model. However, lepton number conservation is not required by Lorentz invariance or gauge invariance, and a number of theoretical extensions to the Standard Model predict lepton-number violation.<sup>4</sup> Many experiments have searched for lepton-number violation in  $K$  decays,<sup>5</sup> and for lepton-number violation and flavor-changing neutral currents in  $D$ <sup>6–11</sup> and  $B$ <sup>12</sup> decays. While many experiments have examined charge 1/3 strange and beauty quarks, investigations of  $D$  mesons look for rare and forbidden decays involving charge 2/3 charm quarks. Charge 2/3 quarks may couple differently than charge 1/3 quarks.<sup>4</sup>

## 2. E791 Analysis

The data were gathered by the the E791 spectrometer,<sup>13</sup> which recorded  $2 \times 10^{10}$  events with a loose transverse energy trigger. These events were produced by a 500 GeV/c  $\pi^-$  beam interacting in a fixed target consisting of five thin, well separated foils. Track and vertex reconstruction was provided by 23 silicon microstrip planes<sup>14</sup> and 45 wire chamber planes plus, two magnets.

Electron identification (ID) was based on transverse shower shape plus matching wire chamber tracks to shower positions and energies in the electromagnetic calorimeter.<sup>15</sup> The electron ID efficiency varied from 62% below 9 GeV to 45% above 20 GeV. The probability to mis-ID a pion as an electron was about 0.8%.

Muon identification was obtained from two planes of scintillation counters. The first plane (5.5 m  $\times$  3.0 m) of 15 counters measured the horizontal  $x$  axis while the second plane (3.0 m  $\times$  2.2 m) of 16 counters measured the vertical  $y$  axis. The counters had about 15 interaction lengths of shielding. Candidate muon tracks were required to pass cuts that were set using  $D^+ \rightarrow \bar{K}^{*0} \mu^+ \nu_\mu$  decays from E791's data.<sup>16</sup> Timing from the  $y$  counters improved  $x$  position resolution. Counter efficiencies were measured using muons originating from the primary beam dump, and were found to be  $(99 \pm 1)\%$  for the  $y$  counters and  $(69 \pm 3)\%$  for the  $x$  counters. The probability for misidentifying a pion as a muon decreased with increasing momentum; from about 6% at 8 GeV/c to  $(1.3 \pm 0.1)\%$  above 20 GeV/c.

After reconstruction,<sup>17</sup> events with evidence of well-separated production (primary) and decay (secondary) vertices were selected to separate charm candidates from background. Secondary vertices had to be separated from the primary vertex by greater than  $20 \sigma_L$  for  $D^+$  decays and greater than  $12 \sigma_L$  for  $D^0$  and  $D_s^+$  decays, where  $\sigma_L$  was the calculated resolution of the measured longitudinal separation. In

addition, the secondary vertex had to be separated from the closest material in the target foils by greater than  $5\sigma'_L$ , where  $\sigma'_L$  was the uncertainty in this separation. The sum of the vector momenta of the tracks from the secondary vertex was required to pass within  $40\text{ }\mu\text{m}$  of the primary vertex in the plane perpendicular to the beam. Finally, the net momentum of the charm candidate transverse to the line connecting the production and decay vertices had to be less than 300, 250, and 200 MeV/ $c$  for  $D^0$ ,  $D_s^+$ , and  $D^+$  candidates, respectively. The decay track candidates passed approximately 10 times closer to the secondary vertex than to the primary vertex. These selection criteria and, where possible, the kaon identification<sup>18</sup> requirements, were the same for the search mode and for its normalization signal.

For this study a “blind” analysis technique was used. Before the selection criteria were finalized, all events having masses within a mass window  $\Delta M_S$  around the mass of  $D^+$ ,  $D_s^+$ , or  $D^0$  were “masked” so that the presence or absence of any potential signal candidates would not bias the choice of selection criteria. All criteria were then chosen by studying signal events generated by a Monte Carlo simulation program (see below) and background events, outside the signal windows, from real data. Events within the signal windows were unmasked only after this optimization. Background events were chosen from a mass window  $\Delta M_B$  above and below the signal window  $\Delta M_S$ . The criteria were chosen to maximize the ratio  $N_S/\sqrt{N_B}$ , where  $N_S$  and  $N_B$  are the numbers of signal and background events, respectively. Asymmetric windows for the decay modes containing electrons were used to allow for the bremsstrahlung low-energy tail. The signal windows were:

- $1.84 < M(D^+) < 1.90\text{ GeV}/c^2$  for  $D^+ \rightarrow h\mu\mu$ ,
- $1.78 < M(D^+) < 1.90\text{ GeV}/c^2$  for  $D^+ \rightarrow hee$  and  $h\mu e$ ,
- $1.95 < M(D_s^+) < 1.99\text{ GeV}/c^2$  for  $D_s^+ \rightarrow h\mu\mu$ ,
- $1.91 < M(D_s^+) < 1.99\text{ GeV}/c^2$  for  $D_s^+ \rightarrow hee$  and  $h\mu e$ ,
- $1.83 < M(D^0) < 1.90\text{ GeV}/c^2$  for  $D^0 \rightarrow \mu\mu$ ,
- $1.76 < M(D^0) < 1.90\text{ GeV}/c^2$  for  $D^0 \rightarrow ee$  and  $\mu e$ .

The sensitivity of the search was normalized to topologically similar Cabibbo-favored decays. For  $D^+$ ,  $24010 \pm 166\text{ } D^+ \rightarrow K^-\pi^+\pi^+$  decays were used; for  $D_s^+$ ,  $782 \pm 30\text{ } D_s^+ \rightarrow \phi\pi^+$  decays were used; and for  $D^0$ ,  $25210 \pm 179\text{ } D^0 \rightarrow K^-\pi^+$  decays were used. The normalization modes widths were  $10.5\text{ MeV}/c^2$  for  $D^+$ ,  $9.5\text{ MeV}/c^2$  for  $D_s^+$ , and  $12\text{ MeV}/c^2$  for  $D^0$ . The upper limit for each branching fraction  $B_X$  was calculated using the following formula:  $B_X = (N_X/N_{\text{Norm}}) \cdot (\varepsilon_{\text{Norm}}/\varepsilon_X) \cdot B_{\text{Norm}}$ , where  $N_X$  was the 90% CL upper limit on the number of decays for rare or forbidden decay mode  $X$ , and  $\varepsilon_X$  was that mode’s detection efficiency.  $N_{\text{Norm}}$  was the fitted number of normalization mode decays;  $\varepsilon_{\text{Norm}}$  was the normalization mode detection efficiency; and  $B_{\text{Norm}}$  was the normalization mode branching fraction obtained from the Particle Data Group.<sup>1</sup>

The ratio of detection efficiencies is given by  $\varepsilon_{\text{Norm}}/\varepsilon_X = N_{\text{Norm}}^{\text{MC}}/N_X^{\text{MC}}$ , where  $N_{\text{Norm}}^{\text{MC}}$  and  $N_X^{\text{MC}}$  are the fractions of Monte Carlo events that are reconstructed and pass final cuts, for the normalization and decay modes, respectively. We use

PYTHIA/JETSET<sup>19</sup> as the physics generator and model effects of resolution, geometry, magnetic fields, multiple scattering, interactions in detector material, detector efficiencies, and analysis cuts. The efficiencies for the normalization modes varied from about 0.5% to 2% and the search modes varied from about 0.1% to 2%.

Monte Carlo studies showed that the experiment’s acceptances are nearly uniform across the Dalitz plots, except that the dilepton identification efficiencies typically dropped to near zero at the dilepton mass threshold. While the loss in efficiency varied channel by channel, the efficiency typically reached its full value at masses only a few hundred MeV/ $c^2$  above the dilepton mass threshold. A constant weak-decay matrix element was used when calculating the overall detection efficiencies. Two exceptions to the use of the Monte Carlo simulations in determining relative efficiencies were made: those for Čerenkov identification when the number of kaons in the signal and normalization modes were different, and those for the muon identification. These efficiencies were determined from data.

### 3. E791 Results

The 90% CL upper limits  $N_X$  were calculated using the method of Feldman and Cousins<sup>20</sup> to account for background, and then corrected for systematic errors by the method of Cousins and Highland.<sup>21</sup> In these methods, the numbers of signal events are determined by simple counting, not by a fit. All results are listed in Table 1 and shown in Fig. 1. The kinematic criteria and removal of reflections (see below) were different for the  $D^+$ ,  $D_s^+$ , and  $D^0$ .

The upper limits were determined by both the number of candidate events and the expected number of background events within the signal region. Background sources that were not removed by the selection criteria discussed earlier included decays in which hadrons (from real, fully-hadronic decay vertices) were misidentified as leptons. In the case where kaons were misidentified as leptons, candidates had effective masses which lie outside the signal windows. Most of these originated from the Cabibbo-favored modes  $D^+ \rightarrow K^- \pi^+ \pi^+$ ,  $D_s^+ \rightarrow K^- K^+ \pi^+$ , and  $D^0 \rightarrow K^- \pi^+$  (and charge conjugates). These Cabibbo-favored reflections were explicitly removed prior to the selection-criteria optimization. There remained two sources of background in the data: hadronic decays with pions misidentified as leptons ( $N_{\text{MisID}}$ ) and “combinatoric” background ( $N_{\text{Cmb}}$ ) arising primarily from false vertices and partially reconstructed charm decays. After selection criteria were applied and the signal windows opened, the number of events within the window was  $N_{\text{Obs}} = N_{\text{Sig}} + N_{\text{MisID}} + N_{\text{Cmb}}$ .

The background  $N_{\text{MisID}}$  arose mainly from singly-Cabibbo-suppressed (SCS) modes. These misidentified leptons can come from hadronic showers reaching the muon counter, decays-in-flight, and random overlaps of tracks from otherwise separate decays (“accidental” sources). A limit for  $D^+ \rightarrow K^- \ell^+ \ell^+$  modes was not attempted, as they had relatively large feedthrough signals from copious Cabibbo-favored  $K^- \pi^+ \pi^+$  decays. Instead, the observed signals in  $K^- \ell^+ \ell^+$  channels were

used to measure three dilepton misidentification rates under the assumption that the observed signals arise entirely from lepton misidentification.

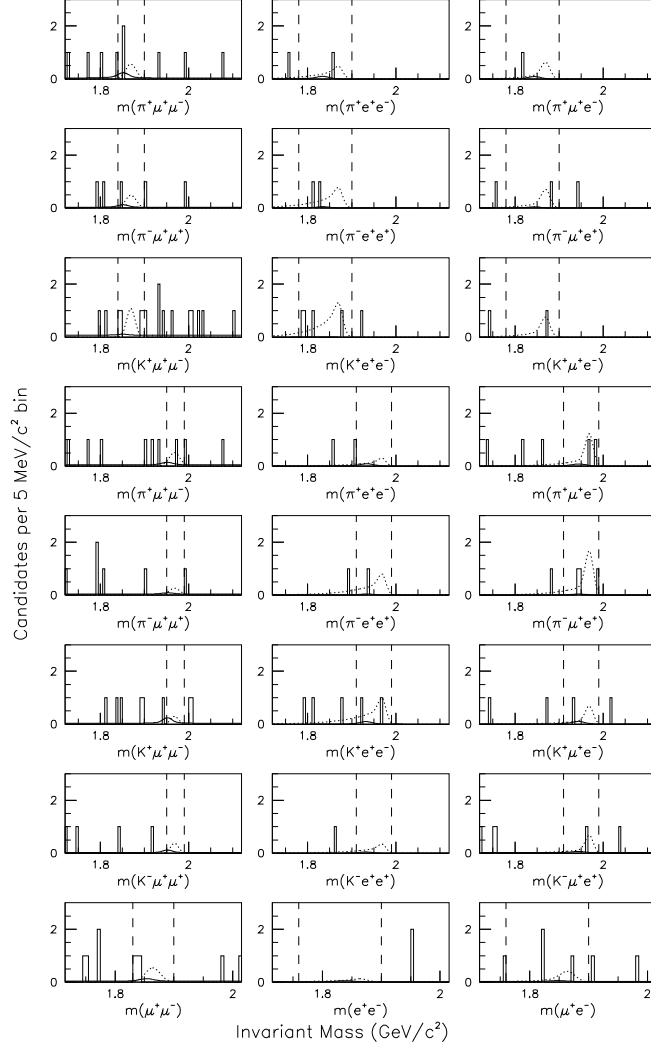


Fig. 1. Final event samples for  $D^+$  (rows 1–3),  $D_s^+$  (rows 4–7), and  $D^0$  (row 8) decays. Solid curves represent estimated background; dotted curves represent signal shape of a number of events equal to a 90% CL upper limit. Dashed vertical lines are  $\Delta M_S$  windows.

The following misidentification rates were obtained:  $r_{\mu\mu} = (7.3 \pm 2.0) \times 10^{-4}$ ,  $r_{\mu e} = (2.9 \pm 1.3) \times 10^{-4}$ , and  $r_{ee} = (3.4 \pm 1.4) \times 10^{-4}$ . Using these rates the numbers of misidentified candidates,  $N_{\text{MisID}}^{h\ell\ell}$  (for  $D^+$  and  $D_s^+$ ) and  $N_{\text{MisID}}^{\ell\ell}$  (for  $D^0$ ), in the signal windows were estimated as follows:  $N_{\text{MisID}}^{h\ell\ell} = r_{\ell\ell} \cdot N_{\text{SCS}}^{h\pi\pi}$  and  $N_{\text{MisID}}^{\ell\ell} = r_{\ell\ell} \cdot N_{\text{SCS}}^{\pi\pi}$ , where  $N_{\text{SCS}}^{h\pi\pi}$  and  $N_{\text{SCS}}^{\pi\pi}$  were the numbers of SCS hadronic

decay candidates within the signal windows. For modes in which two possible pion combinations can contribute, e.g.,  $D^+ \rightarrow \pi^+ \mu^\pm \mu^\mp$ , twice the above rate was used.

To estimate the combinatoric background  $N_{\text{Cmb}}$  within a signal window  $\Delta M_S$ , events having masses within an adjacent background mass window  $\Delta M_B$  were counted, and this number ( $N_{\Delta M_B}$ ) was scaled by the relative sizes of these windows:  $N_{\text{Cmb}} = (\Delta M_S / \Delta M_B) \cdot N_{\Delta M_B}$ . To be conservative in calculating the 90% confidence level upper limits, combinatoric backgrounds were taken to be zero when no events are located above the mass windows. In Table 1 the numbers of combinatoric background, misidentification background, and observed events are presented for all 24 modes. Also previously published results are given for comparison.

Table 1. E791 90% confidence level (CL) branching fractions (BF) compared to previous limits. The background and candidate events correspond to the signal region only.

Mode	(Est. $N_{\text{Cmb}}$ )	BG $N_{\text{MisID}}$	Cand. Obs.	Sys. Err.	90% CL Num.	E791 $BF$ Limit	Previous $BF$ Limit	Ref.
$D^+ \rightarrow \pi^+ \mu^+ \mu^-$	1.20	1.47	2	10%	3.35	$1.5 \times 10^{-5}$	$1.8 \times 10^{-5}$	6
$D^+ \rightarrow \pi^+ e^+ e^-$	0.00	0.90	1	12%	3.53	$5.2 \times 10^{-5}$	$6.6 \times 10^{-5}$	6
$D^+ \rightarrow \pi^+ \mu^\pm e^\mp$	0.00	0.78	1	11%	3.64	$3.4 \times 10^{-5}$	$1.2 \times 10^{-4}$	7
$D^+ \rightarrow \pi^- \mu^+ \mu^+$	0.80	0.73	1	9%	2.92	$1.7 \times 10^{-5}$	$8.7 \times 10^{-5}$	7
$D^+ \rightarrow \pi^- e^+ e^+$	0.00	0.45	2	12%	5.60	$9.6 \times 10^{-5}$	$1.1 \times 10^{-4}$	7
$D^+ \rightarrow \pi^- \mu^+ e^+$	0.00	0.39	1	11%	4.05	$5.0 \times 10^{-5}$	$1.1 \times 10^{-4}$	7
$D^+ \rightarrow K^+ \mu^+ \mu^-$	2.20	0.20	3	8%	5.07	$4.4 \times 10^{-5}$	$9.7 \times 10^{-5}$	7
$D^+ \rightarrow K^+ e^+ e^-$	0.00	0.09	4	11%	8.72	$2.0 \times 10^{-4}$	$2.0 \times 10^{-4}$	7
$D^+ \rightarrow K^+ \mu^\pm e^\mp$	0.00	0.08	1	9%	4.34	$6.8 \times 10^{-5}$	$1.3 \times 10^{-4}$	7
$D_s^+ \rightarrow K^+ \mu^+ \mu^-$	0.67	1.33	0	27%	1.32	$1.4 \times 10^{-4}$	$5.9 \times 10^{-4}$	8
$D_s^+ \rightarrow K^+ e^+ e^-$	0.00	0.85	2	29%	5.77	$1.6 \times 10^{-3}$		
$D_s^+ \rightarrow K^+ \mu^\pm e^\mp$	0.40	0.70	1	27%	3.57	$6.3 \times 10^{-4}$		
$D_s^+ \rightarrow K^- \mu^+ \mu^+$	0.40	0.64	0	26%	1.68	$1.8 \times 10^{-4}$	$5.9 \times 10^{-4}$	8
$D_s^+ \rightarrow K^- e^+ e^+$	0.00	0.39	0	28%	2.22	$6.3 \times 10^{-4}$		
$D_s^+ \rightarrow K^- \mu^+ e^+$	0.80	0.35	1	27%	3.53	$6.8 \times 10^{-4}$		
$D_s^+ \rightarrow \pi^+ \mu^+ \mu^-$	0.93	0.72	1	27%	3.02	$1.4 \times 10^{-4}$	$4.3 \times 10^{-4}$	8
$D_s^+ \rightarrow \pi^+ e^+ e^-$	0.00	0.83	0	29%	1.85	$2.7 \times 10^{-4}$		
$D_s^+ \rightarrow \pi^+ \mu^\pm e^\mp$	0.00	0.72	2	30%	6.01	$6.1 \times 10^{-4}$		
$D_s^+ \rightarrow \pi^- \mu^+ \mu^+$	0.80	0.36	0	27%	1.60	$8.2 \times 10^{-5}$	$4.3 \times 10^{-4}$	8
$D_s^+ \rightarrow \pi^- e^+ e^+$	0.00	0.42	1	29%	4.44	$6.9 \times 10^{-4}$		
$D_s^+ \rightarrow \pi^- \mu^+ e^+$	0.00	0.36	3	28%	8.21	$7.3 \times 10^{-4}$		
$D^0 \rightarrow \mu^+ \mu^-$	1.83	0.63	2	6%	3.51	$5.2 \times 10^{-6}$	$4.1 \times 10^{-6}$	9
$D^0 \rightarrow e^+ e^-$	1.75	0.29	0	9%	1.26	$6.2 \times 10^{-6}$	$8.2 \times 10^{-6}$	10
$D^0 \rightarrow \mu^\pm e^\mp$	2.63	0.25	2	7%	3.09	$8.1 \times 10^{-6}$	$1.7 \times 10^{-5}$	10

The sources of systematic errors in this analysis included: statistical errors from the fit to the normalization sample  $N_{\text{Norm}}$ ; statistical errors on the numbers of Monte Carlo generated events for both  $N_{\text{Norm}}^{\text{MC}}$  and  $N_X^{\text{MC}}$ ; uncertainties in the calculation of misidentification background; and uncertainties in the relative efficiency

for each mode, including lepton and kaon tagging efficiencies. These tagging efficiency uncertainties included: 1) the muon counter efficiencies from both Monte Carlo simulation and hardware performance; 2) kaon Čerenkov identification efficiency due to differences in kinematics and modeling between data and Monte Carlo simulated events; and 3) the fraction of signal events (based on simulations) that would remain outside the signal window due to bremsstrahlung tails. The larger systematic errors for the  $D_s^+$  modes, compared to the  $D^+$  and  $D^0$  modes, are due to the uncertainty in the branching fraction for the  $D_s^+$  normalization mode. The sums, taken in quadrature, of these systematic errors are listed in Table 1.

#### 4. Summary

As demonstrated elsewhere,<sup>3</sup> one can estimate what new mass regions these results can probe. If one, for simplicity, assumes that  $g_{X^0, X'} = g_W$  then for FCNC, using:

$$m_{X^0} \sim m_W \cdot \left[ \frac{BR(D^+ \rightarrow \bar{K}^0 \mu^+ \nu_\mu)}{BR(D^+ \rightarrow \pi^+ \mu^+ \mu^-)} \cdot (2.2) \right]^{1/4}, \quad (1)$$

one estimates that  $m_{X^0} > 800 \text{ GeV}/c^2$ . Applying a similar technique for LFV, and now using the formula:

$$m_{X'} \sim m_W \cdot \left[ \frac{BR(D^+ \rightarrow \bar{K}^0 \mu^+ \nu_\mu)}{BR(D^+ \rightarrow \pi^+ \mu^\pm e^\mp)} \cdot (2.2) \right]^{1/4}, \quad (2)$$

one estimates that  $m_{X'} > 650 \text{ GeV}/c^2$ , consistent with theoretical predictions.<sup>22</sup>

In summary, a “blind” analysis of data from Fermilab experiment E791 was used to obtain upper limits on the dilepton branching fractions for flavor-changing neutral current, lepton-number violating, and lepton-family violating decays of  $D^+$ ,  $D_s^+$ , and  $D^0$  mesons. No evidence for any of these decays was found. Therefore, upper limits on the branching fractions at the 90% confidence level were presented. These limits represent significant improvements over previously published results. Eight new  $D_s^+$  search modes were reported.

For the future, FOCUS (Fermilab experiment E831)<sup>23</sup> will shortly be publishing their results, which should improve on the E791 results. Also, because of interest expressed<sup>24</sup> in resonant decays of  $D^0$ s, Fermilab experiment E791 will shortly be publishing results of a search for  $D^0 \rightarrow V \ell^\pm \ell^\mp$  decays.

#### Acknowledgments

I gratefully acknowledge the assistance of Alan Schwartz for the calculations of the mass regions probed by these rare and forbidden decays. I would also like to express gratitude to Zoltan Ligeti, for inviting me to give the talk at the Fermilab Joint Experimental Theoretical Seminar that was the basis for this review. This research supported under DOE grant DE-FG05-91ER40622.

## References

1. C. Caso et al. (Particle Data Group), *Eur. Phys. J.* **C3**, 1 (1998).
2. E. M. Aitala et al. (Fermilab E791), *Phys. Lett.* **B462**, 401 (1999).
3. A. J. Schwartz, *Mod. Phys. Lett.* **A8**, 967 (1993);  
P. Singer and D.-X. Zhang, *Phys. Rev.* **D55**, 1127 (1997).
4. S. Pakvasa, hep-ph/9705397; S. Pakvasa,  
*Chin. J. Phys. (Taipei)* **32**, 1163 (1994).
5. D. Ambrose et al. (BNL E871), *Phys. Rev. Lett.* **81**, 5734 (1998).
6. E. M. Aitala et al. (Fermilab E791), *Phys. Rev. Lett.* **76**, 364 (1996).
7. P. L. Frabetti et al. (Fermilab E687), *Phys. Lett.* **B398**, 239 (1997).
8. K. Kodama et al. (Fermilab E653), *Phys. Lett.* **B345**, 85 (1995).
9. M. Adamovich et al. (BEATRICE), *Phys. Lett.* **B408**, 469 (1997);  
T. Alexopoulos et al. (Fermilab E771), *Phys. Rev. Lett.* **77**, 2380 (1996).
10. D. Pripstein et al. (Fermilab E789), *Phys. Rev.* **D61**, 032005 (2000).
11. A. Freyberger et al. (CLEO), *Phys. Rev. Lett.* **76**, 3065 (1996).
12. S. Glenn et al. (CLEO), *Phys. Rev. Lett.* **80**, 2289 (1998);  
B. Abbott et al. (D0), *Phys. Lett.* **B423**, 419 (1998);  
F. Abe et al. (CDF) *Phys. Rev.* **D57**, 3811 (1998);  
F. Abe et al. (CDF), *Phys. Rev. Lett.* **76**, 4675 (1996);  
C. Albajar et al. (UA1), *Phys. Lett.* **B262**, 163 (1991).
13. J. A. Appel, *Ann. Rev. Nucl. Part. Sci.* **42**, 367 (1992), and references therein;  
D. J. Summers et al., *XXVII<sup>th</sup> Rencontre de Moriond*, Electroweak Interactions and  
Unified Theories, Les Arcs, France, 417 (15-22 March, 1992), hep-ex/0009015;  
S. Amato et al., *Nucl. Instrum. Meth.* **A324**, 535 (1992);  
E. M. Aitala et al. (Fermilab E791), *Phys. Rev. Lett.* **77**, 2384 (1996);  
E. M. Aitala et al. (Fermilab E791), *Phys. Lett.* **B403**, 185 (1997);  
E. M. Aitala et al. (Fermilab E791), *Phys. Lett.* **B403**, 377 (1997);  
E. M. Aitala et al. (Fermilab E791), *Phys. Rev.* **D57**, 13 (1998);  
E. M. Aitala et al. (Fermilab E791), *Phys. Lett.* **B421**, 405 (1998);  
E. M. Aitala et al. (Fermilab E791), *Phys. Rev. Lett.* **83**, 32 (1999);  
E. M. Aitala et al. (Fermilab E791), *EPJdirect* **C4** 1 (1999).
14. B. R. Kumar, in *Vertex Detectors*, Plenum Press, Erice, 167 (21-26 September 1986).
15. V. K. Bharadwaj et al., *Nucl. Instrum. Meth.* **155**, 411 (1978);  
V. K. Bharadwaj et al., *Nucl. Instrum. Meth.* **A228**, 283 (1985);  
D. J. Summers, *Nucl. Instrum. Meth.* **A228**, 290 (1985).
16. E. M. Aitala et al. (Fermilab E791), *Phys. Lett.* **B440**, 435 (1998).
17. S. Bracker et al., *IEEE Trans. Nucl. Sci.* **43**, 2457 (1996);  
C. Stoughton and D. J. Summers, *Comp. Phys.* **6**, 371 (1992).
18. D. Bartlett et al., *Nucl. Instrum. Meth.* **A260**, 55 (1987).
19. H.-U. Bengtsson and T. Sjöstrand, *Comp. Phys. Commun.* **82**, 74 (1994);  
T. Sjöstrand, *PYTHIA 5.7 and JETSET 7.4 Physics and Manual*, CERN-TH.7112/93,  
1995, hep-ph/9508391.
20. G. J. Feldman and R. D. Cousins, *Phys. Rev.* **D57**, 3873 (1998).
21. R. D. Cousins and V. L. Highland, *Nucl. Instrum. Meth.* **A320**, 331 (1992).
22. M. Leurer, *Phys. Rev. Lett.* **71**, 1324 (1993).
23. P. D. Sheldon, *Proceedings of Heavy Flavors 8*, Southampton, UK (25-29 July 1999),  
hep-ex/9912016.
24. S. Prelovšek, S. Fajfer and P. Singer, *Nucl. Phys. Proc. Suppl.* **75B**, 141 (1999);  
S. Fajfer, S. Prelovšek, and P. Singer, *Phys. Rev.* **D58**, 094038, (1998).